SIMULATION OF NATURAL CONVECTION HEAT TRANSFER USING NANOFLUID IN A CONCENTRIC ANNULUS

by

Keivan FALLAH[a*], Atena GHADERI[b], Nima SEDAGHATIZADEH[c], and Mohammad Hossein BORGHEI[d]

[a] Department of Mechanical Engineering, Sari Branch, Islamic Azad University, Sari, Iran
[b] Department of Mechanical Engineering, Ayatollah Amoli Branch, Islamic Azad University, Amol, Iran
[c] School of Mechanical Engineering, University of Adelaide, Adelaide, Australia
[d] Department of Mechanical Engineering, Iran University of Science and Technology, Tehran, Iran

Original scientific paper
https://doi.org/10.2298/TSCI150118078F

In the present study, natural convection of nanofluids in a concentric horizontal annulus enclosure has been numerically simulated using the lattice Boltzmann method. A water-based nanofluid containing Al_2O_3 nanoparticle has been studied. Simulations have been carried while the Rayleigh number ranges from 10^3 to 10^5 and solid volume fraction varies between 0 and 0.04. The effects of solid volume fraction of nanofluids on hydrodynamic and thermal characteristics such as average and local Nusselt numbers, streamlines, and isotherm patterns for different values of solid volume fraction, annulus gap width ratio and Rayleigh number are investigated and discussed in detail.

Keywords*: natural convection, nanofluid, non-centric annulus, lattice Boltzmann method*

Introduction

The problem of natural convection in annulus between two horizontal cylinders has attracted much attention due to its wide applications in solar collector-receiver, underground electric transmission cables, vapor condenser for water distillation, and food process. The literature survey shows that there is numerous works on both experimental and numerical investigation natural convection heat transfer between two concentric circular cylinders [1-4], *etc.*. Heat transfer enhancement in these systems is of great importance from the industrial and energy saving perspectives. The low thermal conductivity of conventional heat transfer fluids, such as water, is considered a primary limitation in enhancing the performance and the compactness of such thermal systems. An innovative technique to improve the heat transfer is adding the nanoscale particles to the base fluid, which has been used extensively in the past decade [5-11], *etc.* The corresponding results show that the existence of the nanoparticles can reduce or increase the rate of heat transfer based on the geometry and boundary conditions of the problem, type, size, shape, and volume fraction of the nanoparticles. Therefore, the effects of nanofluids on the heat transfer must be studied.

* Corresponding author, e-mail: keyvan.fallah@gmail.com

One of the useful numerical methods that have been used in the recent years is the lattice Boltzmann method (LBM). The LBM has several advantages over other conventional CFD methods due to its particular nature and local dynamics. The major advantages of the LBM are due to the fact that the solution for the particle distribution functions is explicit, easy for parallel computation and implementation of boundary conditions on complex boundaries is simple. It has been used for simulating the flow field in wide ranges of engineering applications such as natural convection [12], nanofluid [13, 14], unsteady flow [15-20], *etc*.

The aim of this study is to investigate heat transfer characteristics of natural convection in the annulus between horizontal concentric cylinders filled with Al_2O_3-water nanofluid. The LBM with single-relaxation-time collision model is employed. The study is carried out at a various range of annulus gap width ratio ($0.5 \leq \sigma \leq 5$) and solid volume fractions (0% to 4%) at Rayleigh numbers 10^3-10^5.

Numerical method

The LB method implemented here is the same as that employed in Fattahi *et al*. [12] and Mei *et al*. [16]. In this work, the most popular model for 2-D problems, the D_2Q_9 model, which consists of nine distribution functions, has been used.

The LBM for the flow field

The LBM solves the microscopic kinetic equation for the particle distribution function $f(x, v, t)$ .These particle distribution functions are normally calculated by solving the following equation:

$$\frac{\partial f}{\partial t} + \vec{\mathrm{V}}\nabla f = \Omega(f) \tag{1}$$

where $\Omega(f)$ is the collision operator.

The LB equation of velocity field with the BGK collision operator and external force can be discretized in space x and time t, into the following form:

$$f_i(\boldsymbol{x} + c_i\Delta t, t + \Delta t) = f_i(\boldsymbol{x}, t) + \frac{\Delta t}{\tau_v}\left[f_i^{\mathrm{eq}}(\boldsymbol{x}, t) - f_i(\boldsymbol{x}, t)\right] + \Delta t\, c_i F_i \tag{2}$$

where F_i is the external force in the direction of lattice velocity, τ_v denotes the lattice relaxation time for the flow field and f_i^{eq} stands for the equilibrium distribution function. The kinematic viscosity, ν, is defined in terms of its respective relaxation time, *i. e.* $3\nu = (\tau_v - 0.5)$.

The equilibrium distribution function, which depends on the local density and velocity, is computed:

$$f_i^{\mathrm{eq}} = w_i\rho\left[1 + \frac{\boldsymbol{c}_i\vec{\mathrm{u}}}{c_s^2} + \frac{1}{2}\frac{(\boldsymbol{c}_i\vec{\mathrm{u}})^2}{c_s^4} - \frac{1}{2}\frac{u^2}{c_s^2}\right] \tag{3}$$

In the eq. (3), w_i and $\boldsymbol{c}_i$ denote the weighting factor and the particle velocity for the i^{th} direction in the discrete velocity space, respectively.

Based on conservation laws of mass and momentum, the macroscopic density, ρ, and velocity, $\vec{\mathrm{u}}$, in terms of the density distribution functions are calculated by:

$$\rho = \sum_{i=0}^{8} f_i \tag{4}$$

$$\rho\vec{\mathrm{u}} = \sum_{i=0}^{8} f_i c_i \tag{5}$$

In order to incorporate buoyancy forces into the model, the force term in eq. (2) needs to be calculated in the vertical direction (y) as:

$$F = 3 w_i \mathrm{g}_y \beta\theta \tag{6}$$

For natural convection the Boussinesq approximation is applied and radiation heat transfer is negligible. To ensure that the code works in a near incompressible regime, the characteristic velocity of the flow for natural, $V_{\mathrm{Natural}} = (\beta \mathrm{g}_y \Delta TH)^{1/2}$ regimes must be small compared with the fluid speed of sound. In the present study, the characteristic velocity was selected as 0.1 of sound speed.

The LB equation for the temperature field

In natural convection problems, the effect of viscous heat dissipation can be neglected for applications in incompressible flow, Mei *et al*. [16]. So, the BGK equation for the temperature field is defined:

$$g_i\left(\boldsymbol{x} + c_i\Delta t, t + \Delta t\right) = g_i\left(\boldsymbol{x}, t\right) + \frac{\Delta t}{\tau_D}\left[g_i^{\mathrm{eq}}\left(\boldsymbol{x}, t\right) - g_i\left(\boldsymbol{x}, t\right)\right] \tag{7}$$

where τ_D denotes the lattice relaxation time for the temperature field. The thermal diffusivity, α, is defined in terms of its respective relaxation time, $3\alpha = (\tau_D - 0.5)$. Furthermore, the local equilibrium distribution function of temperature field is calculated:

$$g_i^{\mathrm{eq}} = w_i T\left[1 + \frac{\vec{\mathrm{c}}_i \cdot \vec{\mathrm{u}}}{c_s^2}\right] \tag{8}$$

Also, the temperature is recovered using the summation on g_i:

$$T = \sum_{i=0}^{8} g_i \tag{9}$$

Curve boundary conditions

In CFD the ability to handle complex geometries accurately and efficiently is the primary discussion. Various methodologies have been proposed for simulating the flow over complex geometries while using LBM. In this work, the method proposed in [14] has been used for treating curved boundaries in the velocity and temperature fields.

The LB method of the nanofluid

Nanofluids have different behavior from pure liquids due to inter-particle potentials and other forces act on them. Therefore, some governing equations should be modified for modeling the nanofluid flows. That is because of changes in the fluid thermal conductivity, density, heat capacitance, and thermal expansion which are discussed in this section.

The thermal diffusivity in nanofluids is given by:

$$\alpha_{\mathrm{nf}} = \frac{k_{\mathrm{nf}}}{(\rho c_p)_{\mathrm{nf}}} \tag{10}$$

The effective density of a nanofluid is written:

$$\rho_{\mathrm{nf}} = (1-\phi)\rho_{\mathrm{nf}} + \phi\rho_{\mathrm{s}} \tag{11}$$

where ϕ is the solid volume fraction of nanoparticles and f, s, and nf denote base fluid, solid nanoparticle, and nanofluid properties, respectively.

The heat capacitance of the nanofluid and thermal expansion coefficient in the Boussinesq equation can be written:

$$(\rho c_p)_{\mathrm{nf}} = (1-\phi)(\rho c_p)_{\mathrm{f}} + \phi(\rho c_p)_{\mathrm{s}} \tag{12}$$

$$(\rho\beta)_{\mathrm{nf}} = (1-\phi)(\rho\beta)_{\mathrm{f}} + \phi(\rho\beta)_{\mathrm{s}} \tag{13}$$

The dynamic viscosity of the nanofluid containing a dilute suspension of small rigid spherical particles is given by Khanafer and Vafai [9]:

$$\mu_{\mathrm{nf}} = -0.4491 + \frac{28.837}{T} + 0.574\phi - 0.1634\phi^2 + 23.053\frac{\phi^2}{T^2} + 0.0132\phi^3 - \\ -2354.735\frac{\phi}{T^3} + 23.498\frac{\phi^2}{d_p^2} - 3.0185\frac{\phi^3}{d_p^2} \tag{14}$$

The thermal conductivity of the nanofluids can also be defined [21]:

$$\frac{k_{\mathrm{nf}}}{k_{\mathrm{f}}} = 1 + 64.7\phi^{0.764}\left(\frac{d_{\mathrm{f}}}{d_{\mathrm{s}}}\right)^{0.369}\left(\frac{k_{\mathrm{f}}}{k_{\mathrm{s}}}\right)^{0.7476}\mathrm{Pr}_T\,\mathrm{Re}_T^{1.2321} \tag{15}$$

where d_{s} and d_{f} are nanoparticles diameter and molecular diameter of fluid, respectively. The Pr_T and Re_T are given by:

$$\mathrm{Pr}_T = \frac{\mu_{\mathrm{f}}}{\rho_{\mathrm{f}}\alpha_{\mathrm{f}}} \quad \text{and} \quad \mathrm{Re}_{\mathrm{T}} = \frac{\rho_{\mathrm{f}} k_b T}{3\pi\mu_{\mathrm{f}}^2 l_{\mathrm{f}}} \tag{16}$$

where l_{f} is the mean path of the fluid particle that is assumed as 17 nm similar to [22] and k_b is the Boltzmann constant. It should be noticed that, this model is based on experimental measurements of Chon *et al*. [22] for Al_2O_3 suspension in water at volume fraction up to 4% and includes the nanoparticle size and the work temperature effects. However, Minsta *et al*. [23] showed that this model is appropriate for thermal conductivity prediction of both Al_2O_3 and Cu nanoparticles up to a volume fraction of 9% by experimental test.

The dimensionless relaxation time for flow and temperature fields which are determined by the nanofluid properties are:

$$\tau_\upsilon = \frac{3}{2}\nu_{\mathrm{nf}(lbm)} + 0.5 \tag{17}$$

$$\tau_D = \frac{3}{2}\alpha_{\mathrm{nf}(lbm)} + 0.5 \tag{18}$$

That *lbm* subscript determines the lattice scale.

Computational domain and numerical details

The physical model of this work is shown in fig. 1. A 2-D horizontal annulus is bounded by an outer radius R_{o} and an inner core radius R_i and θ is measured counterclockwise from

the upward vertical plane through the center of the cylinders. T_h and T_c are the constant temperatures of the inner and outer cylinders, respectively, and $T_h > T_c$. The fluid in the annulus is a water-based nanofluid containing Al_2O_3 or Cu nanoparticles. Also, $\sigma = 2R_i/(R_o - R_i)$ denotes annulus gap width ratio.

In this problem, the Rayleigh number is defined:

$$\mathrm{Ra} = \frac{\mathrm{g}\beta\Delta T\left(R_o - R_i\right)}{\alpha\nu} \tag{19}$$

We assumed that nanofluid is similar a pure fluid and then nanofluid qualities are gotten and they were applied for the equations. The ratio of nanofluid Rayleigh number to that of the base fluid can then be expressed:

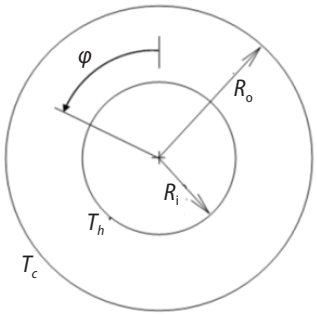

Figure 1. Flow geometry for annulus

$$\frac{\mathrm{Ra}_{\mathrm{nf}}}{\mathrm{Ra}_{\mathrm{f}}} = \frac{\beta_{\mathrm{nf}}}{\beta_{\mathrm{f}}}\frac{\nu_{\mathrm{f}}}{\nu_{\mathrm{nf}}}\frac{\alpha_{\mathrm{f}}}{\alpha_{\mathrm{nf}}} \tag{20}$$

Local Nusselt numbers are named on inner and outer cylinder as Nu_i, Nu_o:

$$\mathrm{Nu}_i = \frac{k_{\mathrm{nf}}}{k_{\mathrm{f}}} R_i \ln\left(\frac{R_o}{R_i}\right)\left.\frac{\partial T}{\partial r}\right|_{r=R_i} \qquad \mathrm{Nu}_o = \frac{k_{\mathrm{nf}}}{k_{\mathrm{f}}} R_o \ln\left(\frac{R_o}{R_i}\right)\left.\frac{\partial T}{\partial r}\right|_{r=R_o} \tag{21}$$

The mean Nusselt number can be calculated:

$$\overline{\mathrm{Nu}} = \frac{k_{\mathrm{nf}}}{k_{\mathrm{f}}}\frac{1}{2\pi}\int_0^{2\pi}\left(\mathrm{Nu}\right)\varphi\,\mathrm{d}\varphi \tag{22}$$

The average Nusselt number is:

$$\mathrm{Nu}_{\mathrm{ave}} = \frac{\overline{\mathrm{Nu}}_o + \overline{\mathrm{Nu}}_i}{2} \tag{23}$$

Results and discussion

In this article the effect of nanoparticle suspension in water is studied for $\mathrm{Ra} = 10^3$-10^5 and solid volume fraction 0 to 0.05. Water is the base fluid with Pr = 6.57 at 22 °C, containing Al_2O_3 nanoparticle. The nanofluid is assumed incompressible and flow is considered to be laminar and 2-D. It is idealized that water and nanoparticles are in thermal equilibrium and non-slip occurs between the two media. Physical and thermal properties of both solid and fluid at the base temperature 20 °C are listed in tab. 1 [6].

In order to prove that the results are independent of the grid size, the numerical results using four different grids are presented in tab. 2 in a case of $\mathrm{Ra} = 10^5$, Pr = 0.71, and $\sigma = 1.25$ with no nanoparticles in the flow field. Four successively grids as 41 × 41, 61 × 61, 81 × 81, and 101 × 101 are tested for grid independence by calculating the average Nusselt number. As shown in tab. 2, it was concluded that a 81 × 81 grid can be considered as a good compromise between accuracy and computational costs. The solution was converged when the relative error between the new and old values of velocity components and temperature fields become less than 10^{-4} and 10^{-8}, respectively.

Table 1. Thermo physical properties of different phases

Property	Fluid phase (water)	Solid phase (Al_2O_3)
c_p [Jkg^{-1}K^{-1}]	4179	765
ρ [kgm^{-3}]	997.1	3970
K [Wm^{-1}K^{-1}]	0.613	25
$\beta \cdot 10^5$[K^{-1}]	21	0.85
d_P [nm]	0.384	47

Table 2. Grid-independent study for the case of Ra = 10^5, and Pr = 0.71

Mesh size	41 × 41	61 × 61	81 × 81	101 × 101
Nu_{ave}	3.28	3.50	3.66	3.71

To validate the present study two different cases are considered. First, natural convection in a cylindrical annulus is simulated at Ra = $4.59 \cdot 10^4$ and σ = 1.25 is considered. Figure 2 shows the obtained streamlines and isotherms lines of the present study in comparison with the experimental results of Guj *et al.* [4]. The comparison indicates that the results have good agreement with experimental data.

Second, the result of heat transfer enhancement in horizontal annuli using nanofluids has been represented. The normalized average Nusselt number at different void fractions are presented in fig. 3 and are compared with the numerical results of Abu-Nada *et al.* [7] and Sheikhzadeh *et al* [8] for Ra = 10^5, σ = 1.25 and Pr = 6.2. The normalized average Nusselt number is defined as the ratio of average Nusselt number at any volume fraction of nanoparticles to that of pure water and is given:

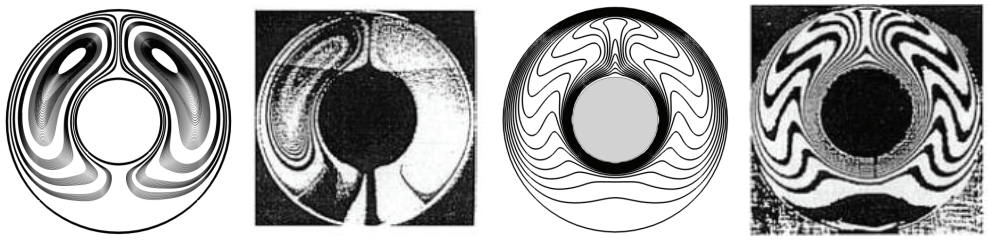

Figure 2. Comparison of streamlines and isotherms lines of the present study and experimental work of Guj *et al.* [4] for Ra = $4.59 \cdot 10^4$, Pr = 0.71, and σ = 1.25

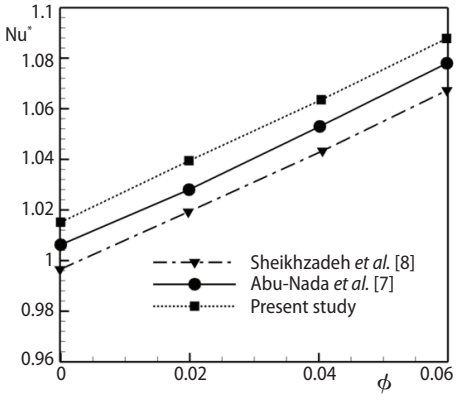

Figure 3. Comparison of present study with numerical results

$$Nu^* = \frac{\overline{Nu}}{\overline{Nu}\big|_{\phi=0}} \tag{24}$$

It can be clearly seen that the present numerical approach is in good agreement with the previous ones.

In order to obtain insight into the detailed flow structures, initially, streamline, and isotherm pattern at different volume fraction, Rayleigh number and annulus gap width ratio for Al_2O_3 is presented in figs. 4 and 5. The streamlines are drawn on the left half of the annulus, while the isotherms are plotted on the right half. Due to the large quantity of data, some results are omitted. Figure 4 illustrates the effects of volume fraction and Rayleigh number on the heat and fluid flow patterns for σ = 0.5. It is clear that by increasing the volume fraction of nanoparticles the maximum strength of streamlines is reduced due to the increased viscosity of the nanoflu-

ids. Also, the figures show that the thickness of the thermal boundary layer decreases with increasing the volume fraction. It is due to the increase in heat conduction which is associated with the presence of the nanofluid. As the volume fraction increases, irregular and random movements of particles increase the energy exchange rates in the fluid. Also, it can be seen that at low Rayleigh number (10^3) the fluid flow in the half-annuals is weak and forms a symmetrical re-circulation. In this condition, the isotherms are nearly concentric indicating the small effect of the convective flow on heat transfer rate. As Rayleigh number increases, the fluid motion becomes stronger and center of rotation moves upward. Also, a radial temperature inversion appears, indicating separation of the inner and outer boundary layers by increasing Rayleigh number.

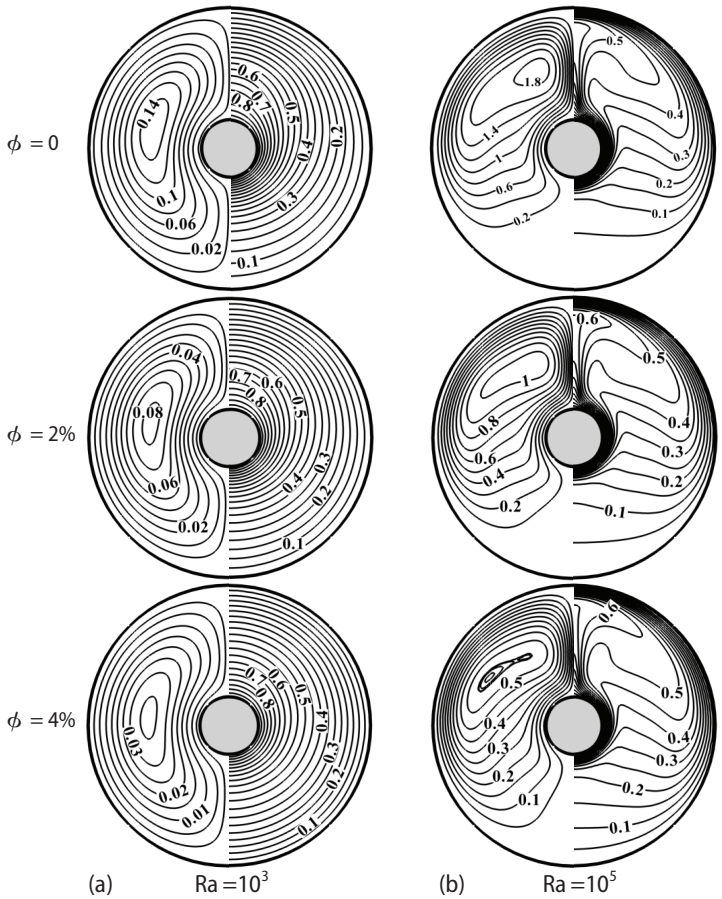

Figure 4. Streamlines and isotherm pattern at: (a) Ra = 10^3, and (b) Ra = 10^5 at different volume fractions for σ = 0.5

Figure 5 presents the influence of the annulus gap width ratio on the heat and fluid flow patterns within the concentric annulus at fixed volume fraction (φ = 0.02) of Al_2O_3 nanoparticles for Ra = 10^3 and 10^5. At Ra = 10^3, heat transfer is mainly due to conduction since the fluid motion driven by the buoyancy force is very slow. As shown in figs. 5(a) and 5(b), the isotherms form concentric circles and center of rotation is the midpoint of the annulus that is due to the conduction domination in these cases. In fig. 5(c), the results show that the center of rotation of the flow is in the top portion of the annulus, and the isotherms form eccentric circles due to the strong convection heat transfer, where σ = 1. As the annulus gap width ratio increases, the flow becomes weaker, and the center of rotation moves toward the midpoint of the annulus, and the isotherms form concentric circles as shown in fig. 5(d). The effect of the annulus gap width ratio can be described as follows; for a small gap width ratio, the thickness of the velocity boundary layers is less than the gap between the cylinders. Consequently, a free stream velocity exists in the gap leading to an increase in the radial and tangential velocity components. Hence, as shown in fig. 5(c), the possibility of developing a thermal boundary layer will increase and the cold fluid moves to the lower part of the annulus and hot fluid moves to a the upper part

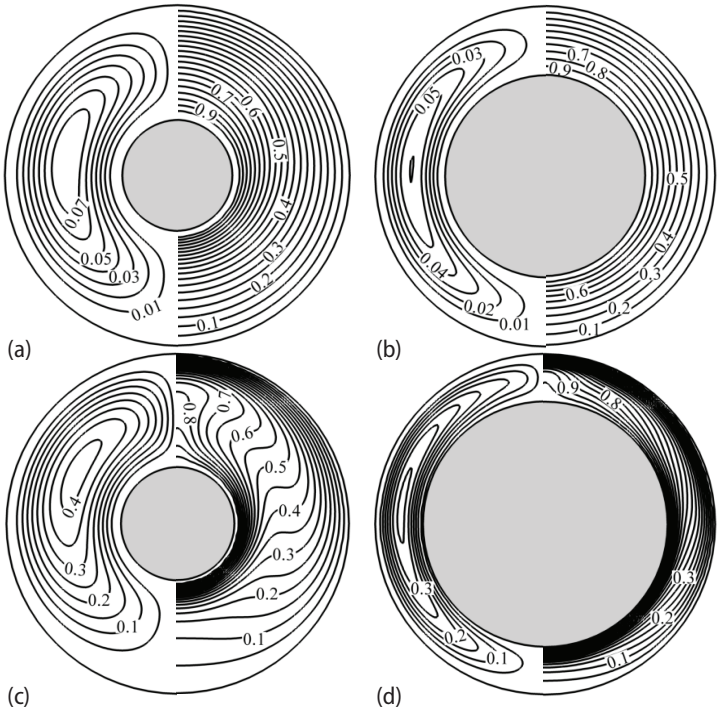

Figure 5. Streamlines and isotherm pattern at: (a) Ra = 10^3, σ = 1, (b) Ra = 10^3, σ = 3, (c) Ra = 10^5, σ = 1, and (d) Ra = 10^5, σ = 5 with volume fractions ϕ = 0.02

of it due to natural convection. As the annulus gap width ratio is augmented, the influence of the viscosity becomes higher. Hence, the thickness of the velocity boundary layers is wider than the gap between the cylinders. Consequently, the thermal boundary layer will decrease due to reduce in the radial and tangential velocity components and this causes the fluid between the inner and outer surfaces behave similar to a solid insulating material.

The local Nusselt number distribution is one of the important parameters in the present study, since it can reflect the local heat transfer characteristics around the inner and outer cylinder.

Hence, the local Nusselt number distribution at various Rayleigh number, σ, and ϕ for Al_2O_3 nanoparticle are presented in figs. 6 and 7. Figure 6 illustrates how the addition of nanoparticles influences the Nusselt number distribution around inner and outer cylinder for different Rayleigh numbers at various volume fractions of Al_2O_3 nanoparticles when σ = 0.5. It is observed that Nusselt number increases with the increasing of Rayleigh number, as expected. It is due to elevation buoyancy forces, which augments thermal convective currents.

The effect of the annulus gap width ratio on the local Nusselt number along the inner and outer cylinder at Ra = 10^5 and ϕ = 2% is shown in fig. 7. Over the range of annulus gap width ratio, the Nusselt number of the inner (outer) cylinder starts from a local minimum (maximum) at φ = 0 (top of the annulus) and then increases (decreases) to the point φ = 180 (at the bottom), indicating that the convection heat transfer is dominant. In the case of σ = 5, because of the conduction effect, the local Nusselt number curve shows no remarkable change around the inner cylinder and it is specially seen for the outer surface.

For better discussion, the values of the averaged Nusselt numbers *vs.* volume fractions of Al_2O_3-water nanofluid at different annulus gap width ratios for Ra = 10^3, 10^4, and 10^5 are shown in figs. 8(a), (b), and (c), respectively. Also, the diagrams show that the mean Nusselt number decreases with increasing the annulus gap width ratio. The maximum decrease in the mean Nusselt numbers is seen for Ra = 10^5. Increment of Rayleigh number strengthens the fluid motion and consequently affects the temperature field, creating a higher temperature gradient which leads to a higher Nusselt number for all cases.

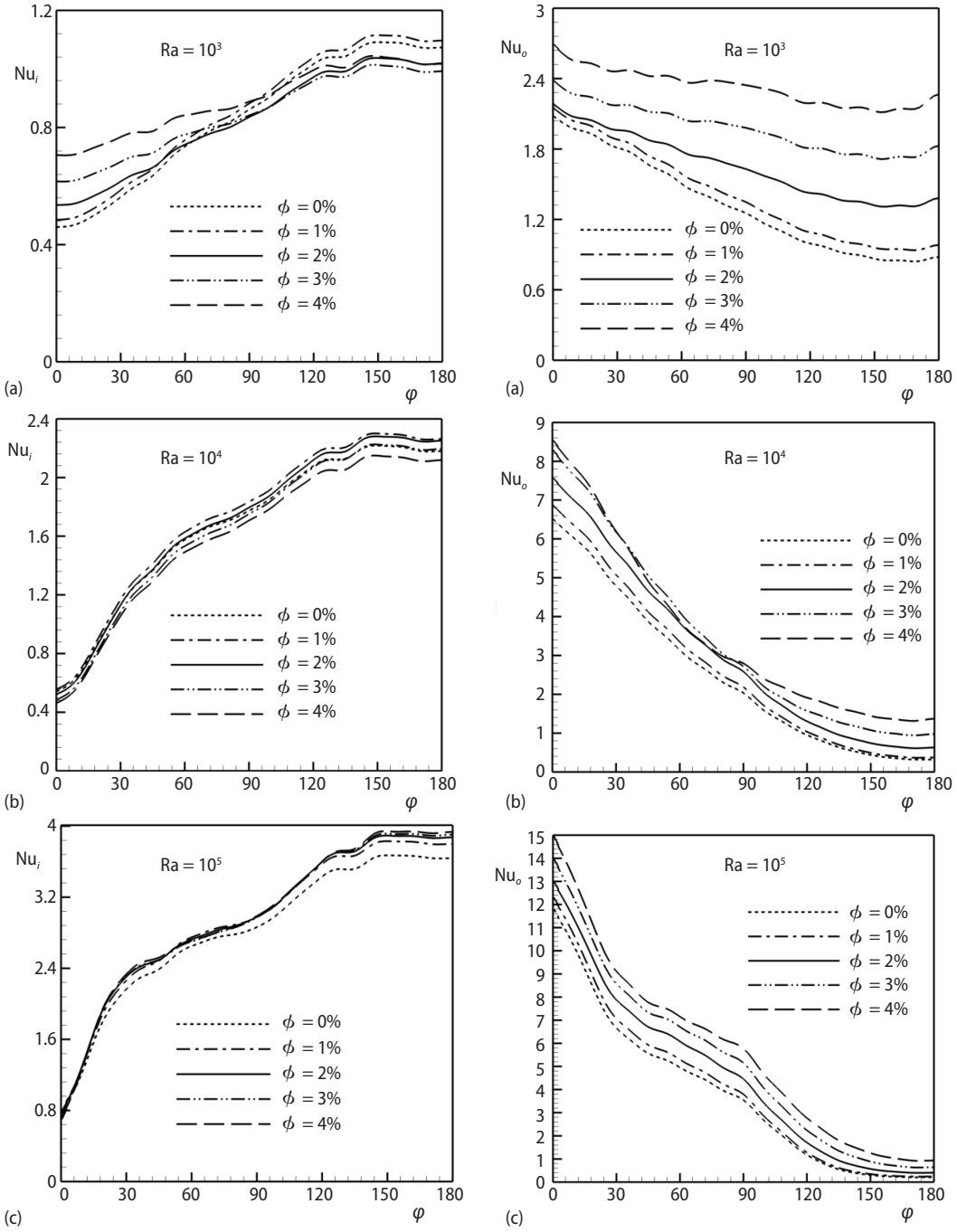

Figure 6. Local Nusselt number distribution around inner (left) and outer (right) cylinder at various volume fractions of Al_2O_3 nanoparticles at: (a) Ra = 10^3, (b) Ra = 10^4, and (c) Ra = 10^5 for $\sigma = 0.5$

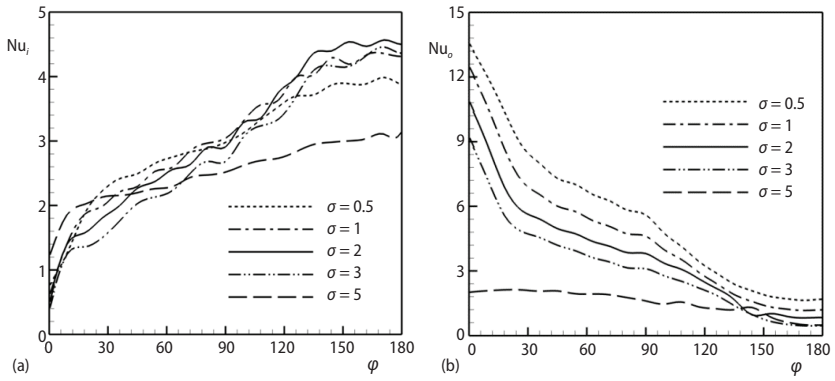

Figure 7. Local Nusselt number distribution around inner (a) and outer (b) cylinder at Ra = 10^5, and ϕ = 2% for different annulus gap width ratio

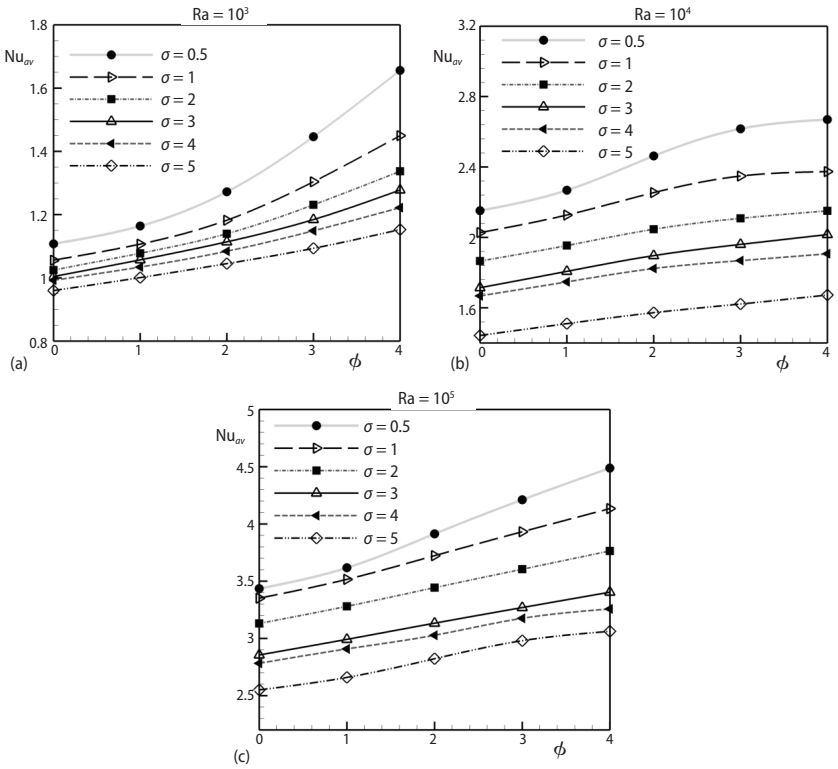

Figure 8. Average Nusselt number *vs.* to volume fraction for Al_2O_3-water nanofluid at different annulus gap width ratio for: (a) Ra = 10^3, (b) Ra = 10^4, and (c) Ra = 10^5

Conclusions

Natural convection flow utilizing nanofluids in a horizontal annulus enclosure was simulated numerically using the LBM. The results are presented as Rayleigh numbers vary between 10^3 to 10^5 and the annulus gap width ratio ranges as $0.5 \leq \sigma \leq 5$ containing Al_2O_3

nanoparticle while solid volume fractions vary from 0% to 4%. The conclusion of the present study can be summarized as follows.

- It is found that LBM is a suitable approach for simulating natural convection using nanofluid in the geometry which includes curved boundaries. The simple implementation of efficient thermal conductivity is the most preference of this method.
- As solid volume fraction increases in the annulus, the Nusselt number at the both outer and inner cylinder increases.
- Results show that the mean Nusselt number decreases with increasing the annulus gap width ratio at the same Rayleigh number.
- By increasing solid volume fraction, the results show a heat transfer enhancement at any Rayleigh number.
- In all the cases considered volume fraction and gap-width ratio, the mean Nusselt number augments with increasing the Rayleigh number.

Nomenclature

c – lattice speed, [ms^{-1}]
c_p – specific heat capacity, [JK^{-1}kg^{-1}]
c_s – speed of sound, [ms^{-1}]
d_P – diameter of solid particles, [m]
F – external force, [N]
f – distribution function for flow field, [–]
g – distribution function for temperature, [–]
g_y – acceleration due to gravity, [ms^{-2}]
H – height, [m]
k – thermal conductivity, [WK^{-1}m^{-1}]
Nu – local Nusselt number, [–]
Nu_i – inner local Nusselt number, [–]
$\underline{Nu}_o$ – outer Local Nusselt number, [–]
$\overline{Nu}$ – mean Nusselt number, [–]
Pr – Prandtl number, [–]
Ra – Rayleigh number, [–]
Re – Reynolds number, [–]
T – macroscopic temperature, [K]
t – time, [s]
u – velocity in the x-direction, [ms^{-1}]
v – velocity in the y-direction, [ms^{-1}]
w – weight function, [–]

Greek symbols

α – thermal diffusivity, [m^{2}s^{-1}]
β – thermal expansion coefficient, [–]
θ – dimensionless temperature, [–]
μ – viscosity, [kgm^{-1}s^{-1}]
ν – kinematic viscosity, [m^{2}s^{-1}]
ρ – fluid density, [kgm^{-3}]
σ – annulus gap width ratio, [–]
τ – relaxation time, [s]
τ_D – lattice relaxation time, [s]
φ – tangential direction, [–]
ϕ – volume fraction, [–]

Subscripts

ave – average
c – low temperature
f – fluid
h – high temperature
i – direction of single-particle
l – local
nf – nanofluid
p – particle
s – solid

Superscripts

eq – equilibrium

Acronyms

BGK – Bhatnagar-Gross-Krook operator
LBM – lattice Boltzmann method

References

[1] Kuehn, T., Goldstein, R., An Experimental and Theoretical Study of Natural Convection in the Annulus between Horizontal Concentric Cylinders, *J. Fluid Mech., 74* (1976), 4, pp. 695-719
[2] Kuehn, T., Goldstein, R., A Parametric Study of Prandtl Number and Diameter Ratio Effects on Natural Convection Heat Transfer in Horizontal Cylindrical Annuli, *J. Heat Transfer*, *102* (1978), 4, pp.768-770
[3] Glakpe, E. K., *et al.*, Constant Heat Flux Solutions for Natural Convection between Concentric and Eccentric Horizontal Cylinders, *Numer. Heat Transfer*, *10* (1986), 3, pp. 279-295
[4] Guj, G. S., *et al.*, Experimental Analysis of Thermal Fields in Horizontally Eccentric Cylindrical Annuli, *Exp. Fluid.*, *12* (1992), 6, pp.385-393

[5] Choi, S. S., Enhancing Thermal Conductivity of Fluids with Nanoparticles, in: *Developments and Application of Non-Newtonian Flows*, (Eds. D. A. Siginer, H. P. Wang), ASME, New York, USA, Vol. 231, pp 99-105
[6] Oztop, H. F., Abu-Nada, E., Numerical Study of Natural Convection in Partially Heated Rectangular Enclosures Filled with Nanofluids, *Int. J. Heat Fluid Flow*, *29* (2008), 5, pp. 1326-1336
[7] Abu-Nada, E., *et al.*, Natural Convection Heat Transfer Enhancement in Horizontal Concentric Annuli Using Nanofluids, *Int. Commun. Heat Mass Transfer*, *35* (2008), 5, pp. 657-665
[8] Sheikhzadeh, G. A., *et al.*, Laminar Natural Convection of Cu-Water Nanofluid in Concentric Annuli with Radial Fins Attached to the Inner Cylinder, *Int. J Heat Mass Tran., 49* (2013), 3, pp. 391-403
[9] Khanafer, K., Vafai, K., A Critical Synthesis of Thermophysical Characteristics of Nanofluids, *International Journal of Thermal Sciences*, *49* (2010), 19-20, pp. 2339-2352
[10] Salari, M., *et al.*, Mixed Convection of Nanofluid Flows in a Square Lid-Driven Cavity Heated Partially from both the Bottom and Side Walls, *Numerical Heat Transfer, Part A, 62* (2012), 2, pp. 158-177
[11] Salari, M., *et al.*, Numerical Solutions to Heat Transfer of Nanofluid Flow over Stretching Sheet Subjected to Variations of Nanoparticle Volume Fraction and Wall Temperature, *Appl. Math. Mech.-Engl. Ed., 35* (2014), 1, pp. 63-72
[12] Fattahi, E., *et al.*, Lattice Boltzmann Simulation of Mixed Convection Heat Transfer in Eccentric Annulus, *Int. Communc. Heat Mass., 38* (2011), 8, pp. 1135-1141
[13] Nemati, H., *et al.*, Lattice Boltzmann Simulation of Nanofluid in Lid-Driven Cavity, *Int. J. Heat Mass Transfer*, *37* (2010), 10, pp. 1528-1534
[14] Nemati, H., *et al.*, Magnetic Field Effects on Natural Convection Flow of Nanofluid in a Rectangular Cavity Using the Lattice Boltzmann Model, *Scientia Iranica, 19* (2012), 2, pp. 303-310
[15] Fattahi, E., *et al.*, Lattice Boltzmann Simulation of Natural Convection Heat Transfer in Nanofluids, *Int. J. Thermal Sci., 52* (2012), Feb., pp. 137-144
[16] Mei, R., *et al.*, Force Evaluation in the Lattice Boltzmann Method Involving Curved Geometry, *Phys. Rev. E, 65* (2002), Apr., 041203
[17] Fallah, K., *et al.*, Multiple-Relaxation-Time Lattice Boltzmann Simulation of Non-Newtonian Flows Past a Rotating Circular Cylinder*, J Non-Newton Fluid*, *177-178* (2012), June, pp. 1-14
[18] Fallah, K., *et al.*, Numerical Simulation of Planar Shear Flow Passing a Rotating Cylinder at Low Reynolds Numbers, *Acta Mech., 223* (2012), 2, pp. 221-236
[19] Fallah, K., *et al.*, Simulation of Planar Shear Flow Passing Two Equal Sized Circular Cylinders in Tandem Arrangement, *Proceedings*, AIP Conference, Antalya, Turkey, Vol. 1400, 2011, pp. 449-452
[20] Yan, Y. Y., Zu, Y. Q., Numerical Simulation of Heat Transfer and Fluid Flow Past a Rotating Isothermal Cylinder a LBM Approach, *Int., J. of Heat and Mass Tran., 51* (2008), 9-10, pp. 2519-2536
[21] Saha, L. K., *et al.*, Effect of Hall Current on the MHD Laminar Natural Convection Flow from a Vertical Permeable Flat Plate with Uniform Surface Temperature, *Int. J. Thermal Sci*., *46* (2007), 8, pp. 790-801
[22] Chon, C. H., *et al.*, Empirical Correlation Finding the Role of Temperature and Particle Size for Nanofluid (Al_2O_3) Thermal Conductivity Enhancement, *Appl. Phys. Lett., 87* (2005), 15, 153107
[23] Minsta, H. A., *et al.*, New Temperature and Conductivity Data for Water-Based Nanofluids, *Int. J. Thermal Sci.*, *48* (2009), 2, pp. 363-371

Paper submitted: January 18, 2015
Paper revised: April 23, 2015
Paper accepted: May 2, 2015